Pergamon

Cement and Concrete Research 30 (2000) 481–489

CEMENT AND CONCRETE RESEARCH

Effect of carbonates on the corrosion rate of cement mortars in nitric acid

V. Pavlík*

Slovak University of Technology, Faculty of Civil Engineering, Department of Material Engineering, Radlinského 11, 813 68 Bratislava, Slovak Republic

Received 4 August 1999; accepted 4 January 2000

Abstract

The rate of corrosion of cement pastes and mortars containing additional finely ground limestone, silica fume, travertine sand, quartz sand or glass balls in a solution of nitric acid were studied. The corrosion process was monitored by visual inspection and by measuring the depth of corrosion, mass loss, and shrinkage of the layers of the corrosion products. It was found that adding finely ground limestone to cement pastes increased the rate of corrosion. In contrast, the rate of corrosion of cement mortars made from travertine sand was the slowest of all test samples and seemed to decrease in relation to the particle size of travertine.

Keywords: Corrosion; Cement paste; $CaCO_3$; Mortar; Acid

1. Introduction

Acid solutions are among the most aggressive media for damaging concrete. The most aggressive acids (in regards to concrete corrosion) seem to be those that produce easily soluble calcium salts, such as nitric, hydrochloric or acetic acid [1–3]. The acids react with hydrated cement compounds and residues of unhydrated cement. During an acid attack, the prevailing calcium ions are leached out by the aggressive solution. A mass of the less soluble corrosion products remains on the surface of the specimen, where it forms a soft and porous decalcified corrosion layer [1–20]. It is usually clearly distinguishable from the still unaffected or slightly affected part of the hardened cement paste (HCP) underlying it. The corrosion layer is composed predominantly of amorphous hydrated Si, Al, and Fe oxides [1–16], with small residual amounts of CaO and MgO. At a sufficiently low pH, the hydrated oxides of iron (at pH $\leq$ 2) and aluminum (at pH $\leq$ 4) also dissolve and pass into the solution [1–5,14]. Temporary existence of aluminate complexes may occur, especially in the vicinity of the uncorroded part of the specimen. The existence of such compounds was reported by Chandra [5], Madrid et al. [15] and Israel et al. [16]. These additional compounds were reported to disappear later as a result of decreasing pH and were not found in an amorphous surface layer.

Below, the layer of corrosion products (the so-called external corrosion layer) with almost no adherence, the so-called internal or "core" layer was reported to exist in some cases [12,15,16]. From this internal layer, the portlandite crystals were removed by leaching.

During corrosion, the H^+ ions or acid molecules are predominantly transported by diffusion across the porous barrier of the layer of corrosive products to the relatively thin reaction zone inside the specimen, where they are consumed. Diffusion (of H^+ ions across the corrosion layer), as the slowest state of the corrosion process, controls the rate of corrosion [1–4,14,18,19]. The change in the permeability of the uncorroded part of the specimen is not thought to have an effect on the process of acid corrosion [3]. The rate of corrosion is affected by the type of acid and other factors; it increases with the concentration of acid [1,3,4,10,17a–19] and also slightly with the water-to-cement (W/C) ratio [4,9,10,14]. A contrasting view is presented by Fattuhi and Hughes [23].

Silica fume and/or fly ash are mostly reported to have only a little or no effect on the durability performance of concrete and cement mortars when they are under the attack of acid solutions [2,9,11,13–20]. It is explained by the fact that, in the course of an acid attack, the H^+ ions or molecules of an acid diffuse only through the porous layer of the decalcified corrosion products. Therefore, the silica fume is assumed to affect the corrosion resistance of the cement

* Tel.: +421-7-59274-691; fax: +421-7-52494-357.
E-mail address: pavlik@svf.stuba.sk (V. Pavlík).

0008-8846/00/$ – see front matter
PII: S0008-8846(00)00201-5

matrix composite only indirectly (and insignificantly [3,20]) by changing the diffusion resistance of the layer of decalcified corrosion products. Nischer [24,25], on the contrary, claims that the acid resistance of high-performance concrete with W/C ratios of about 0.35 is improved by the addition of microsilica. We conclude that the positive effect of microsilica reported by Nischer [25,26] was due mainly to the lower W/C ratio of the concrete with the microsilica; the effect of microsilica was rather small if concrete, with an equal W/C ratio were compared.

Carbonates, e.g., limestone, dissolve in the acidic solutions. Information about the corrosion of cement matrix composites containing carbonaceous aggregate is scarce. According to Harrison [21] "The presence of limestone aggregate in concrete will increase the overall vulnerability of the concrete to attack by acid. Under certain circumstances however, where very small but highly acidic quantities of acid are generated but with low pH as instanced by condensation on the walls of sewerage above the effluent [22], a large amount of neutralizing hard limestone aggregate has been shown to prolong the life of the construction." Nischer [24] reported that "In the case of the high performance concrete with carbonaceous aggregate, the damage was greater than in the case of high performance concrete with quartzitic aggregate." The reason for this, according to Nischer, "is that in the case of concrete with carbonaceous aggregate not only the HCP is dissolved, but also the aggregate and, in particular, the fines."

The effect of adding limestone filler on the properties of cement composites has been extensively studied worldwide. The addition of limestone has been found to improve the sulfate resistance of cement composites, such as those containing cement with higher C_3A content. This effect has been mostly related to the possible chemical reaction of calcium carbonate with C_3A, or eventually, C_4AF during the hydration of cement with the subsequent formation of a low form of calcium carboaluminate hydrate $3CaO{\cdot}Al_2O_3{\cdot}CaCO_3{\cdot}11-12H_2O$ [26–29]. Attacking acids, however, decompose phases of HCP and also calcite. Therefore, the eventual formation of carboaluminate complex(es) in cement pastes is not expected to affect the acid resistance of cement composites.

2. Experimental

2.1. Materials

2.1.1. Cement

Portland cement was used. Its chemical composition is given in Table 1. The mineralogical composition of the cement was: C_3S (56.35%), C_2S (12.24%), C_3A (10.18%), C_4AF (9.67%).

2.1.2. Finely-ground limestone (L in figures)

The basic properties are shown in Table 1. The distribution of the particle size of the finely-ground limestone used was determined by a Laser Particle Sizer (Fig. 1). The color of the ground limestone was white.

2.1.3. Crushed travertine (T)

Crushed waste rocks from the travertine quarry in the locality of Dreveník-Spisské Podhradie (in Slovakia) were used. The basic properties of crushed travertine are shown in Table 1. The main mineral was calcite. Narrow fractions of the travertine sand were obtained from the crushed travertine by sieving. Cement mortars with two different grades of travertine sand were prepared. The grading of travertine sand used is given in Fig. 1. The color of travertine was pale-brown.

2.1.4. Natural silica sand (Q)

Narrow fractions were separated from standard silica (quartz) sand by sieving. Cement mortars with three different grades of quartz sand were prepared. The grading of

Table 1
Composition and physical properties of the materials used

Chemical composition	Portland cement (%)	Silica fume (%)	Finely-ground limestone (%)	Crushed travertine (%)
Insoluble residue	2.13	–	–	–
Fe_2O_3	3.18	1.10	–	0.31
Al_2O_3	5.87	0.80	–	0.81
CaO	62.42	3.30	54.07	52.17
MgO	1.37	1.70	1.51	1.17
SiO_2	19.10	above 90	–	2.92
SO_3	1.85	–	–	0.51
Loss on ignition	2.22	1.36	44.07	41.86
Free lime	0.82	–	–	–
S^{2-}	–	0.11	–	–
Density [kg m^{-3}]	3140	2200	2627	2816
Apparent density [kg m^{-3}]	–	–	–	2482[a]
Porosity [%]	–	–	–	11.85[b]
Specific surface area [m^2 kg^{-1}]	340	19000	–	–

[a] Determined on an aggregate fraction of 8–32 mm.
[b] Calculated value from the density and apparent density of an aggregate fraction of 8–32 mm.

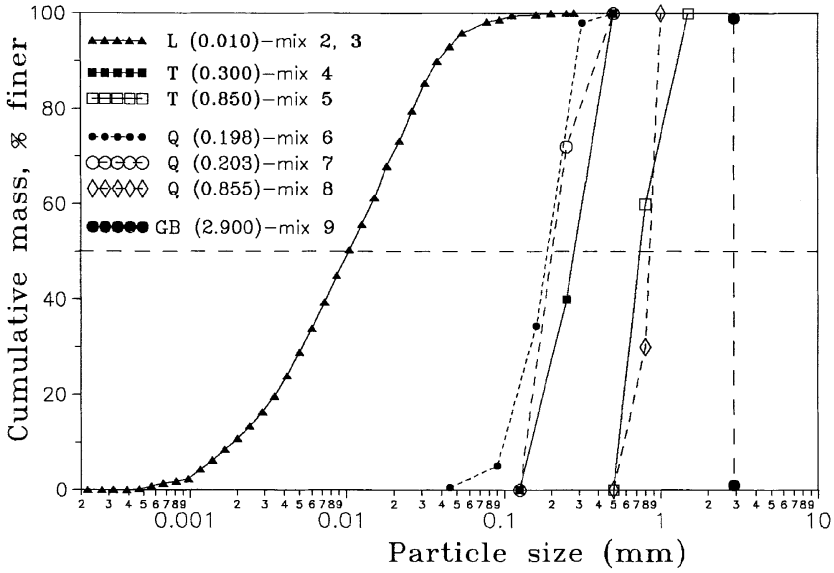

Fig. 1. The particle size distribution of finely-ground limestone (L), travertine (T) and quartz (Q) sands used and the size of the glass balls (GB). The medians of particle sizes of limestone and weight average of the particle sizes of quartz and travertine sands are in parentheses. The weight average of particle sizes of quartz and travertine sands were calculated using the formula:

$$D_A = \frac{D_1 + D_2}{2}\frac{p_{1,2}}{100} + \frac{D_2 + D_3}{2}\frac{p_{2,3}}{100} + \cdots \frac{D_{n-1} + D_n}{2}\frac{p_{n-1,n}}{100}$$

where D_A is weight average size (diameter) of a sand; $D_1, D_2, \ldots D_{n-1}, D_n$ are the lower and upper sieve sizes of the sand fractions; $p_{1,2}, \ldots p_{n-1,n}$ are percentages by mass of the sand fractions.

sands used is given in Fig. 1. The density of quartz sand was 2635 kg m^{-3}. The sand contained over 98% of SiO_2.

2.1.5. Silica fume (SF)

Silica fume was a by-product of the production of silicon. Its chemical composition and selected properties are shown in Table 1.

2.1.6. Glass balls (GB)

The laboratory glass balls (glass beads) were of equal size, with a diameter (d) of 2.9 mm and a density (ρ) of 2510 kg m^{-3}. The chemical composition of glass balls was: SiO_2 (64.0%), B_2O_3 (2.5%), Al_2O_3 (5.0%), Na_2O (15%), CaO (7.0%), MgO (1.5).

2.1.7. Nitric acid solution

The nitric acid solution was prepared with a concentration of 0.2 mol/l; the pH value of the solution was about 0.7.

2.2. Preparation of the specimens and the test procedure

Five types of test specimens were prepared as follows: (a) control specimens made of plain cement paste (later designated as hardened cement paste or "HCP specimens"); (b) specimens of pastes made from laboratory-prepared blended cements containing finely-ground limestone powder; (c) specimens of cement mortars containing quartz sand (mixture no. 6 of quartz mortar also contained additional silica fume); (d) specimens of cement mortars containing travertine sand (mortars with two different grades of the travertine sand were prepared); and (e) specimens of cement composites containing glass balls (glass ball composites). In this article, the term "cement mortar" will also refer to the cement matrix composite containing glass balls. The composition of the dry mixtures is shown in Table 2. The W/C of all pastes and mortars was kept constant at 0.5. The consistency of cement pastes and mortars was therefore different.

The test specimens were prepared using glass tubes that were filled with cement paste, cement mortars or glass ball composites. Three specimens with the same composition were prepared from each batch. The specimens were consolidated by a slight tapping. The inner diameters of the tubes were 3.2 or 1.4 cm; the tubes were open on only one side. The specimens were cured for 24 h at 20°C and 100% relative humidity and then in lime water for another 27 days. Finally, they were placed into an aggressive solution of nitric acid. The concentration of the acid solution was maintained at a constant value (c = 0.2 mol/l). All specimens in the aggressive solution were hung vertically on a string, with the reaction surface facing upward. The depth of corrosion of the specimens was measured regularly during the experiment using callipers. The depth of corrosion was defined as the distance between the end of a glass tube (the surface of the specimen before corrosion) and the boundary between the corroded and uncorroded part of the specimen. The boundary was clear-cut and visually recognisable; the corroded part was almost white with a thin rust-brown ring

Table 2
Proportions of the components in dry mixtures. The medians (*) or weighted averages of particle sizes (mm) of materials used are in parentheses

Mixture no.	Designation	Proportions of components (by weight)					
		Finely-ground limestone	Travertine sand	Quartz sand	Glass balls	Silica fume	Cement
1	HCP-I	–	–	–	–	–	1
2	L-5/2	0.8 (0.010)*	–	–	–	–	1
3	L-6	0.5 (0.010)*	–	–	–	–	1
4	T-10	–	1 (0.300)	–	–	–	1
5	T-12	–	1 (0.850)	–	–	–	1
6	QSF-7	–	–	1 (0.198)	–	0.2	1
7	Q-11	–	–	1 (0.203)	–	–	1
8	Q-14	–	–	1 (0.855)	–	–	1
9	GB-2	–	–	–	1 (2.90)	–	1

adjacent to the grey, uncorroded part of the specimen. In addition to the depth of corrosion, shrinkage of the corroded layers and mass loss of specimen with reference to the constant reaction area were also determined regularly by weighing the specimens. The shrinkage of the corroded layer was measured as the distance between the end of the glass tube and the external surface of the corroded specimen (or as the difference between the depth of the corrosion and the thickness of the corroded layer). It also was measured using callipers.

3. Results and discussion

A layer of corrosion products was observed forming on the surface of specimens early during the first day of immersion of the test specimens in the solution of nitric acid. The thickness of the corroded layer rapidly increased over time. The colour of the corroded cementitious material changed across the corroded layer. It was white (light brown only in the case of specimens containing travertine) in the external zone adjacent to the surface of the corroded layer; underneath, it turned into a thin rust-brown zone. The white-coloured part of the layer consisted mostly of $SiO_2 \cdot aq$; the rust-brown colour related to the presence of Fe (III) compounds ($Fe_2O_3 \cdot aq$) in the deeper zone. The content of CaO in the corroded cementitious material of all the specimens was less than about 1–3%.

A visual inspection of the partially corroded specimen of HCP (control specimen from mixture no. 1) revealed long cracks running perpendicularly across the layer of corrosion products. Cracks in the corroded layer of specimen with glass balls (mixture no. 9) spread radially around the glass balls. The cracks developed as a result of volume contraction of the cementitious material in the process of its decalcification and conversion into a mass of corrosive products. The corroded layers of cement mortars containing quartz sand (mixture nos. 6–8) did not contain any visible cracks running across the corroded layers. Fine cracks were noticed only on the surface of corroded layers. The formation and chemical composition of the various zones in the layer of corrosion products as well as the chemical composition of the specimens itself generally corresponded to the results that were presented in several studies [1,3–20] and photographically documented for example in Refs. [3,5,20].

The layers of corrosion products covering the surface of cement pastes containing finely-ground limestone powder (mixture nos. 2 and 3) formed a compact homogenous mass. Their appearance did not visually differ from that of the HCP (mixture no. 1); these layers of the corrosion products were also pervaded with long cracks. However, no such cracks were noticed in the corroded layers of cement mortars containing travertine sand (mixture nos. 4 and 5). The corroded layers of travertine mortars had a porous, cellular-like appearance. They contained large holes (pores) that remained after the travertine sand particles were dissolved in acid. Calcite (and similarly, $MgCO_3$) dissolved according to the following chemical reaction:

$$CaCO_3 + 2H^+ \rightarrow Ca^{2+} + H_2O + CO_2$$

The shape and size of these large holes corresponded to the space and geometry of the travertine grains that originally occupied the mortars. Fig. 2 shows the detailed photographs of fragments of the corroded layer and the uncorroded part of the mortar that contain travertine sand (mixture no. 5).

The decalcification of the cementitious material led to the volume contraction (shrinkage) of corroded layers of all specimens. The shrinkage of the layers of corrosion products, expressed in percentages of the depth of corrosion by length (in a direction perpendicular to the surface of specimens), is shown in Table 3. As could be expected, the corroded layers of cement mortars containing the inert (siliceous) filling materials, i.e., quartz sand or glass balls (mixture nos. 6–9), shrank less than the corroded layers of HCP specimens (no. 1) and the specimens containing carbonates (nos. 2–5). The shrinkage of the corroded layers of travertine mortars seemed to increase with the particle size of travertine grains. The shrinkage of the corroded layer of each particular specimen did not change significantly during the duration of the experiment. However, in the early stages of corrosion, the depth of corrosion, and the true values of shrinkage in millimeters, were relatively low and they, therefore, could not be measured with the sufficient precision by the method used.

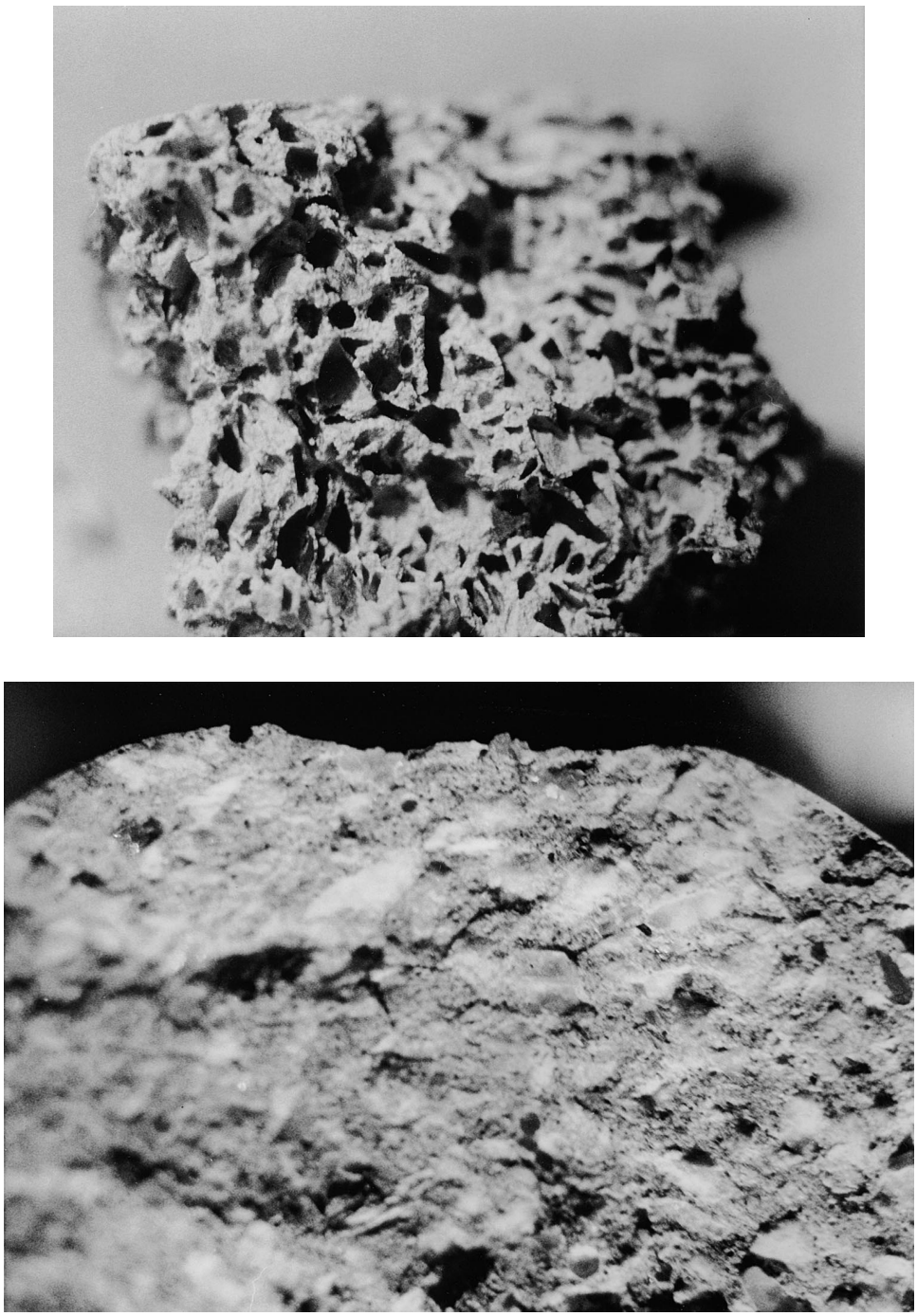

Fig. 2. Effect of the acid attack on cement mortar containing travertine sand (mixture no. 5). The travertine sand was composed of two fractions of 0.5–0.8 mm (60%) and 0.8–1.5 mm (40%). (a) The fragment of the corroded layer with holes that were left after travertine particles were dissolved. (b) The uncorroded part of travertine mortar with intact travertine grains.

The increase in the depth of corrosion of test specimens, which was related to the duration of the attack of nitric acid solution, is presented in Fig. 3. Fig. 3 shows that the rate of corrosion of the test specimen was affected very significantly by the type and chemical composition of mineral admixture and/or sand, and in case of carbonates, also by their grading (Fig. 4).

Cement pastes and mortars containing the inert (with respect to nitric acid) noncarbonaceous components, i.e., the quartz sand, glass balls and also silica fume, corroded with the slower rate rather than the control specimen of HCP. There was very small difference among the corrosion rate of these type of specimens (mixture nos. 6–9). The incorporation of quartz sand reduced the corrosion rate of cement

Table 3
Shrinkage of the corroded layers after 300 days of corrosion

Mixture	1	2	3	4	5	6	7	8	9
Designation	HCP-1	L-5/2	L-6	T-10	T-12	QSF-7	Q-11	Q-14	GB-2
Shrinkage (% by length)	11.7	12.3	10.9	9.3	13.0	6.3	5.0	4.9	5.6

mortars more than the incorporation of glass balls. These findings are in agreement with those reported previously in Ref. [20]. The addition of silica fume did not seem to have a significant effect on corrosion rate. These findings are in agreement with those that were reported by other authors [2,9,11,13–20].

The corrosion of composites containing carbonates, as presented in Figs. 3 and 4, revealed that the rate of corrosion of these specimens decisively depended on the size of carbonaceous components. The pastes containing finely ground limestone (mixture nos. 2 and 3) corroded at the fastest rate; they even corroded more rapidly than the control specimens of HCP (no. 1). The rate of corrosion seemed to increase slightly with the content of finely ground limestone. Cement mortars containing the travertine sand (mixture nos. 5 and 6) corroded more slowly than the specimens containing the ground limestone (nos. 2 and 3) and also the control specimen of HCP (no. 1). The corrosion rate of these specimens decreased with the size of travertine particles.

The type of test specimens (glass tubes with only one open side) permitted the continual measurement of mass loss referred to the constant reaction area. The mass of the samples decreased during the corrosion (Fig. 5). There was a significant difference between the samples. Mass losses increased with the content of calcium in a unit volume of a particular specimen. Therefore, the mass losses of the test specimens that contained carbonates were higher than that of control specimens of HCP (mix no. 1). In contrast, the mass losses of mortars containing quartz sand, silica fume and glass balls were smallest.

We have to mention here that we took the depth of corrosion of the test specimens, and not the loss of mass, as the appropriate criterion for evaluating the damage to specimens (or the degree of corrosion). The reason for adopting this criterion was that it is actually the reduction in thickness (or cross-sectional area) of the undamaged material that determines the amount of damage.

The losses of mass, expressed in grams per unit reaction area (g/cm^2), were linearly proportional to the depth of corrosion of the specimens (Fig. 6). The linearity of these relationships suggests that the cementitious material of a particular specimen (and also a carbonate if a sample contained it) had been decomposed to about the same degree across the entire corrosion layer during corrosion. The mass losses corresponding to a depth of corrosion of 10 mm, therefore, relate to the decomposition of a volume unit (1 cm^3) of the constituting material(s) of a particular specimen (Fig. 6). Moreover, the loss of mass of a particular specimen is approximately proportional to the quantity of acid needed for decomposing a unit volume (1 cm^3) of the specimen. The exact proportionality relates to the molar proportions.

A straight line that expresses the decomposition of the HCP specimen (mixture no. 1) in Fig. 6 divides the bunch

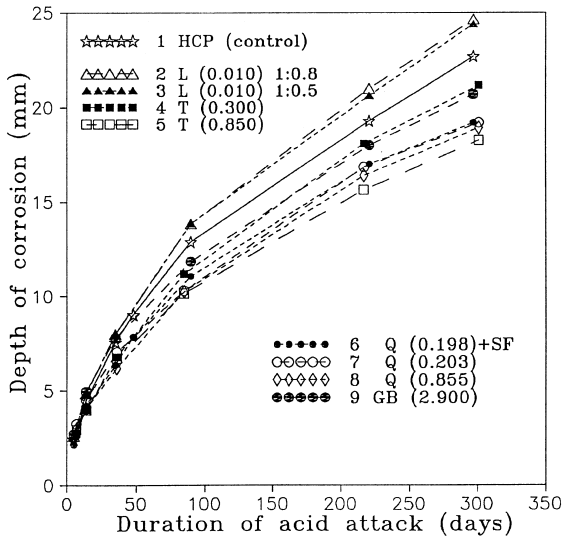

Fig. 3. Corrosion of test specimens related to the duration of the attack by nitric acid solution. The symbols in the legend denote mixture numbers 1–9, abbreviations for hardened cement paste (HCP), limestone (L), travertine (T), quartz (Q), silica fume (SF) and glass balls (GB). The medians and weight average particle sizes are in parentheses.

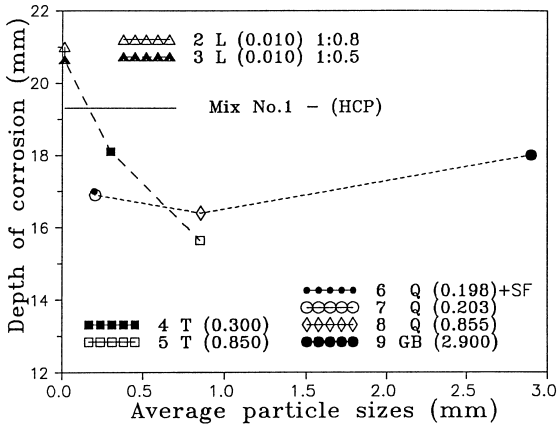

Fig. 4. Depth of corrosion of the test specimens after 210 days of attack by nitric acid related to the particle size of the components used.

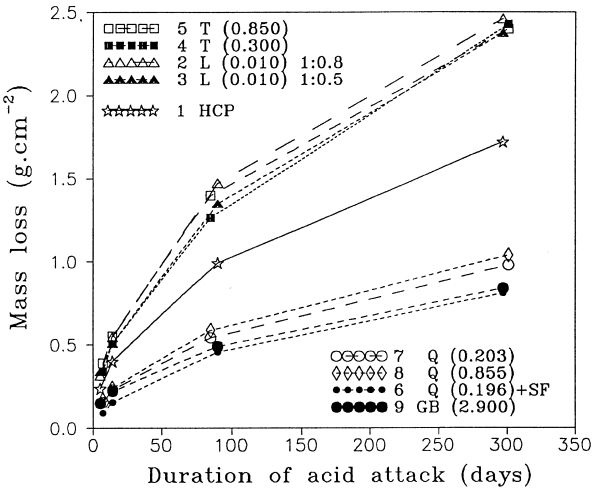

Fig. 5. Mass losses of the test specimens related to the duration of the attack of nitric acid.

of a fan spreading lines into two groups. Into the first group belong the lines of the specimens that contain quartz sand, silica fume and glass balls, i.e., the components that are inert with respect to nitric acid. The second group comprises of the lines belonging to specimens that contain the carbonates (limestone and travertine). The mass losses (referred to the depth of corrosion) of specimens from the first group were smaller than in the second group. The differences among the slopes of lines belonging to the first group may be referred to the differences in density of filling materials, and therefore, also to differences in their volumes. The proportion of volume that is occupied by the inert filling material is smaller, while the proportion of volume occupied by cementitious material is greater. The differences among the slopes of lines in the second group are mainly caused by the different carbonate content in a particular sample. Also, the difference between the density of the ground limestone and travertine is significant. A slightly different slope between the two lines belonging to specimens containing travertine sand of different sizes (mixture nos. 4 and 5) could not be explained.

The visual inspection of the corroded layers of specimens containing carbonates indicated that the carbonate particles were dissolved throughout the entire volume of corroded layers, up to the vicinity of a boundary between the corroded and uncorroded part of specimens. The low pH in the layer of corrosive products is supposed to be responsible for the dissolution of calcium carbonates. According to the findings reported previously [12], the pH value across almost the entire layer of the corrosion products of a neat cement paste sample were substantially lower than 7, until up to the thin reaction zone adjacent to the uncorroded part of the specimen. Only then, in the furthermost boundary zone of the layer of corrosion products, was a steep increase in the pH values observed. Taking this into account, the dissolution of calcium carbonate particles is expected to start at the time when the decalcification (dissolution) front reaches them. After the decalcification front passes by, and the carbonaceous particles dissolve, the empty pores filled with the liquid phase are left behind. The corroded layer of specimens with carbonates is, therefore, more porous than the corroded layers of other specimens, and also, it is supposed to have lower a diffusion coefficient. The quantity of the acid (H^+ ions) required to decompose a unit volume of HCP or mortar is, as was said before, approximately proportional to the leachable calcium content in the constituting materials. The approximate content of CaO in 1 cm^3 of a specimen can be calculated from the composition of a specimen, its W/C ratio, and density of components. Calculations of this type were described in Ref. [14]. For HCP (mixture no. 1), the calculated content of calcium oxide was about 0.76 g CaO/cm^3, while for cement paste containing the finely ground limestone (mixture no. 3), it was about 0.89 g CaO/cm^3 and for pure limestone a with density of 2627 kg/m^3, it was about 1.473 g CaO/cm^3.

These results show that the quantity of acid that is required for the decomposition of a volume unit of paste no. 3 (containing finely ground limestone) is higher compared to the quantity for decomposing a volume unit of the neat cement paste (no. 1). Despite this fact, the rate of corrosion of the specimen (no. 3) is faster than that of HCP (no. 1). These two apparently controversial facts confirm, that in the case of specimens nos. 2 and 3, the dominant factor that controls the rate of corrosion is the diffusion coefficient of the corroded layer, and not the neutralisation capacity of the material constituting the specimen. In other words, the effect of the easier transport of aggressive components across the corroded layer of specimens with the finely ground limestone surpasses the effect of a higher neutralisation capacity of these samples. The various binding of calcium into CSH-phases (or other phases of hydrated cement) and calcite can affect the local dissolution of these

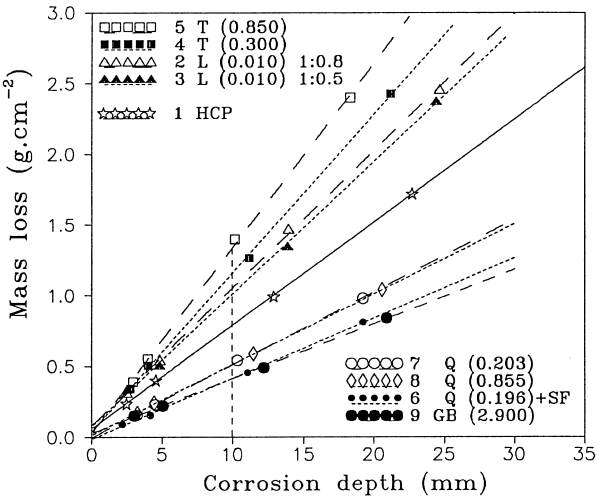

Fig. 6. Mass loss of corroded specimens referred to corrosion depth.

phases. Because the particles of ground limestone are very fine and evenly distributed, the effect of the eventual difference between the rate of dissolution of the different phases seems to be negligible.

In the case of samples that contain travertine with much bigger grains, this conclusion is no longer valid. The particle size of carbonates in these specimens acts as a third factor. Therefore, it is likely that the rate of corrosion, in this case, is affected also by the rate of dissolution of large travertine grains. In addition, travertine has a higher neutralisation capacity than limestone due to its greater density. This fact is also confirmed by the higher values of the mass loss of specimen nos. 4 and 5 (Fig. 6).

The specimens were dried after the corrosion test; then, the cellular layer of the corrosion products of specimen no. 5 was removed, and the surface of the uncorroded material underneath was brushed in order to remove the remaining soft material. The brushed surface of the uncorroded material was rough in contrast to the smooth surfaces under the corroded layer of the control sample of HCP and the samples of pastes with finely ground limestone. An examination of the brushed surface by an optical microscope showed grains of travertine that slightly protruded from the surrounding cement binder. A side view of the brushed sample revealed a light-grey zone in the binding material of up to 3 mm thick that was located under the outer edge of the brushed surface. This zone corresponds to the "core layer" described in Refs. [12,16], which relates to the slightly affected binding material containing amorphous C-S-H, but lacking portlandite. These observations confirmed that the binding material around travertine particles as well as closely under them was affected by the acid's action. This suggests that travertine grains dissolved from the side of their solid surfaces that was facing the incoming acid, but the binding cementitious material was continually decomposing in the thicker reaction zone. Additionally, we might expect that, in the case of an equal diffusion flow of acid to the local surface of the travertine grain and the local surface of the binding material, equal diffusion flows of corrosion products (Ca^{2+}) also exist in the opposite direction. Because the concentration of calcium in the unit volume of travertine prevails above that in the unit volume of the binding material, the dissolution rate of the travertine grain has to be lower. Consequently, the local rate of dissolution of travertine is also expected to be lower than that of the binding material.

4. Conclusions

The development of corrosion of cement pastes and mortars of various composition in the solution of nitric acid was studied. The depth of corrosion of the test specimens was chosen as a convenient parameter for evaluating the extent of corrosion damage. On the basis of the test results, the following conclusions are drawn.

1. The specimen of a neat HCP corrode at a faster rate than the specimens of cement mortars that contain quartz sand (with or without admixture of silica fume) or glass balls. However, the neutralisation capacity and mass loss of the specimen of neat cement paste was higher compared to that of mortars with siliceous sand or other components. These facts relate to smaller proportion of cementitious material in a unit volume (1 cm^3) of these mortars.

2. The specimens of cement pastes and mortars that contain carbonates have a higher neutralisation capacity than the specimens of the neat cement paste and cement mortars containing quartz sand, silica fume and glass balls. They also lose mass with a faster rate than mortars with the siliceous components. In spite of this, the specimens of cement pastes that contained finely ground limestone had the fastest corrosion rate of all specimens.

3. Cement mortars that contain travertine sand had the slowest corrosion rate of all specimens. The rate of corrosion decreased with the size of travertine sand. Travertine grains seem to dissolve at a slower rate than the binding material in the reaction zone.

4. The rate of corrosion of specimens containing carbonates seems to decrease with the size of carbonate particles.

References

[1] I. Biczók, Concrete Corrosion, Protection of Concrete, Verlag der Ungarischen Akademie der Wissenschaften, Budapest, 1960 (in German).
[2] V.M. Moskvin, T.V. Rubetskaya, G.V. Ljubarskaya, Concrete corrosion in acidic media and methods for its investigation, Beton Zhelezobeton (Moscow) (in Russian), 10 (1971) 10–12.
[3] V.M. Moskvin, F.M. Ivanov, S.N. Alexejev, E.A. Gusejev, Corrosion of Concrete and Reinforced Concrete: Methods for their Protection, Strojizdat, Moscow, 1980 (in Russian).
[4] L. Rombén, Aspects on Testing Methods for Acid Attack on Concrete. CBI forskning research 1:78 (und 9:79), Cement-och betong instituted, Stockholm, 1978.
[5] S. Chandra, Hydrochloric acid attack on cement mortar—an analytical study, Cem Concr Res 18 (2) (1988) 193–203.
[6] E. Revertegat, C. Richet, P. Gégout, Effect of pH on the durability of cement pastes, Cem Concr Res 22 (2/3) (1992) 259–272.
[7] A. Delagrave, M. Pigeon, É. Revertégat, Influence of chloride ions and pH level on the durability of high performance cement pastes, Cem Concr Res 24 (8) (1994) 1433–1443.
[8] L. De Ceukelaire, The effect of hydrochloric acid on mortar, Cem Concr Res 22 (5) (1992) 903–914.
[9] A. Bajza, Corrosion of hardened cement paste by NH_4NO_3 and acetic and formic acids, in: L.R. Roberts, J.P. Skalny (Eds.), Pore Structure and Permeability of Cementitious Materials, Mater Res Soc Symp Proc, Vol. 137, Published by Mater Res Soc, Pittsburgh, Pennsylvania 15237, 1989, pp. 325–334.
[10] A. Bajza, Corrosion of hardened cement pastes in formic acid solutions, Proceedings of 9th International Congress on the Chemistry of Cement, NCCB, New Delhi, Vol. V, 1992, pp. 402–408.
[11] A. Bajza, I. Rouseková, S. Uncík, Corrosion of hardened cement paste by acetic and formic acids, Slovak J Civ Eng 2 (4) (1994) 26–34.
[12] V. Pavlík, Corrosion of hardened cement paste by acetic and nitric acids: Part II. Formation and chemical composition of the corrosion products layer, Cem Concr Res 24 (8) (1994) 1495–1508.

[13] S. Uncík, A. Bajza, I. Rouseková, Corrosion rate of hardened cement paste by formic acid, Slovak J Civ Eng 4 (3/4) (1996) 22–27.
[14] V. Pavlík, Corrosion of hardened cement paste by acetic and nitric acids: Part III. Influence of water/cement ratio, Cem Concr Res 26 (3) (1996) 475–490.
[15] J. Madrid, J.M. Diez, S. Goni, A. Macias, Durability of ordinary portland cement and ground granulated blast furnace slag cement in acid medium, Proceedings of 10th International Congress on the Chemistry of Cement, Gothenburg, Sweden Vol. 4, 1997 p. 4iv040.
[16] D. Israel, D.E. Macphee, E.E. Lachovski, Acid attack on pore reduced cements, J Mater Sci 32 (1997) 4109–4116.
[17a] H. Grube, W. Rechenberg, Betonabtrag durch chemisch angreifende saure Wässer, Beton 37 (11) (1987) 446–451.
[17b] H. Grube, W. Rechenberg, Betonabtrag durch chemisch angreifende saure Wässer, Beton 37 (112) (1987) 495–498.
[18] H. Grube, W. Rechenberg, Durability of concrete Structures in acidic waters, Cem Concr Res 19 (5) (1989) 783–792.
[19] H. Grube, U. Neck, Concrete resistant to chemical attack, Concr Precasting Plant Technol 1 (1996) 122–130.
[20] V. Pavlík, S. Uncík, The rate of corrosion of hardened cement pastes and mortars with additive of silica fume in acids, Cem Concr Res 27 (11) (1997) 1731–1745. Erratum: Cem Concr Res 28 (6) (1998) 936–938.
[21] W.H. Harrison, Durability of concrete in acidic soils and waters, Concrete (London) 21 (2) (1987) 18–24.
[22] South African Council for Scientific and Industrial Research, Corrosion of Concrete Sewers, Series DR12, (cited in Ref. [19]).
[23] N.I. Fattuhi, P.B. Hughes, The performance of cement paste and concrete subjected to sulfuric acid attack, Cem Concr Res 18 (4) (1988) 545–553.
[24] P. Nischer, Pipes and manhole bottom parts from high performance concrete, Concr Precasting Plant Technol 12 (1995) 103–119.
[25] P. Nischer, High performance concrete-workability, strength, E-modulus-resistance against dissolution attack, Concr Precasting Plant Technol 3 (1994) 68–77.
[26] K.D. Ingram, K.E. Daugherty, A review of limestone addition to portland cement and concrete, Cem Concr Compos 12 (1991) 165–170.
[27] I. Soroka, N. Setter, The effect of fillers on strength of cement mortars, Cem Concr Res 7 (4) (1977) 449–456.
[28] I. Soroka, N. Stern, Effect of calcareous fillers on sulfate resistance of portland cement, Am Ceram Bull 55 (6) (1976) 594–595.
[29] H.J. Kuzel, H. Pöllmann, Hydration of C_3A in the presence of $Ca(OH)_2$, $CaSO_4$ and $CaCO_3$, Cem Concr Res 21 (5) (1991) 885–895.